Developmental Biology 320 (2008) 446–455

Contents lists available at ScienceDirect

Developmental Biology

journal homepage: www.elsevier.com/developmentalbiology

Nuclear regulator Pygo2 controls spermiogenesis and histone H3 acetylation

Mahalakshmi Nair [a,1], Ippei Nagamori [b,1], Peng Sun [a,1], Durga Prasad Mishra [b,1], Catherine Rhéaume [a], Boan Li [c], Paolo Sassone-Corsi [b,*], Xing Dai [a,d,*]

[a] Department of Biological Chemistry, University of California, Irvine, CA 92697, USA
[b] Department of Pharmacology, University of California, Irvine, CA 92697, USA
[c] School of Life Sciences, Xiamen University, Xiamen, Fujian 361005, PR China
[d] Developmental Biology Center, University of California, Irvine, CA 92697, USA

ARTICLE INFO

Article history:
Received for publication 5 October 2007
Revised 28 May 2008
Accepted 28 May 2008
Available online 6 June 2008

Keywords:
Pygo2
Pygopus
Spermatogenesis
Spermiogenesis
Wnt/β-catenin signaling
Chromatin
Histone acetylation
Testis
Germ cells

ABSTRACT

Mammalian spermiogenesis, a process where haploid male germ cells differentiate to become mature spermatozoa, entails dramatic morphological and biochemical changes including remodeling of the germ cell chromatin. Proteins that contain one or more plant homeodomain (PHD) fingers have been implicated in the regulation of chromatin structure and function. Pygopus 2 (Pygo2) belongs to a family of evolutionarily conserved PHD finger proteins thought to act as co-activators of Wnt signaling effector complexes composed of β-catenin and LEF/TCF transcription factor. Here we analyze mice containing hypomorphic alleles of *pygopus 2* (*Pygo2* or *mpygo2*) and uncover a β-catenin-independent involvement of the Pygo2 protein in spermiogenesis. Pygo2 is expressed in elongating spermatids at stages when chromatin remodeling occurs, and block of Pygo2 function leads to spermiogenesis arrest and consequent infertility. Analysis of spermiogenesis in *Pygo2* mutants reveals reduced expression of select post-meiotic genes including protamines, transition protein 2, and H1fnt, all of which are required for germ cell chromatin condensation, and drastically altered pattern of histone H3 hyperacetylation. These findings suggest that Pygo2 is involved in the chromatin remodeling events that lead to nuclear compaction of male germ cells.

Introduction

The canonical Wnt signaling cascade is required for development and homeostasis of a large array of tissues, and its mis-regulation causes a number of diseases including cancer (Clevers, 2006; Logan and Nusse, 2004). A key event in this signaling pathway is the stabilization and accumulation of β-catenin (Logan and Nusse, 2004). β-catenin translocates into the nucleus, where it forms a complex with the LEF/TCF transcription factor as well as other co-activators such as the Pygopus family of proteins to regulate gene expression (Jessen et al., in press). *Drosophila* Pygopus was originally identified as a highly specific and obligatory component of canonical Wg signaling (Belenkaya et al., 2002; Kramps et al., 2002; Parker et al., 2002; Thompson et al., 2002). Recent gene knockout studies of mammalian *pygopus* homologs support an involvement of *Pygo2* in Wnt signaling in select mammalian tissues, although its function in eye development is Wnt-independent (Li et al., 2007; Schwab et al., 2007; Song et al., 2007). Pygopus proteins contain a PHD finger at their C-termini, a domain through which the protein is able to interact with β-catenin via the adaptor protein Legless/BCL9. Several studies suggest that by virtue of this ability to bind β-catenin, Pygopus proteins act as devoted co-activators and/or facilitate nuclear retention of the β-catenin/LEF/TCF complex (Kramps et al., 2002; Krieghoff et al., 2006; Stadeli and Basler, 2005; Thompson, 2004; Townsley et al., 2004). Importantly, β-catenin-independent association of *Drosophila* Pygo with LEF/TCF target genes has also been reported (de la Roche and Bienz, 2007).

Mammalian spermiogenesis is a post-meiotic process during which haploid male germ cells differentiate and undergo remarkable structural and biochemical transformations to become mature spermatozoa. During mid-late spermiogenesis, spermatids elongate their nuclei, cease transcription, and dramatically remodel their chromatin (Kimmins and Sassone-Corsi, 2005). Somatic histones are displaced from the chromatin by germ cell-specific DNA packaging proteins protamine 1 (Prm1) and 2 (Prm2), resulting in a highly condensed chromatin configuration. The importance of protamines are underscored by the findings that disturbances in histone–protamine displacement associate with infertility in a large number of male patients (Balhorn et al., 1988; Chevaillier et al., 1987; de Yebra et al., 1993), and that genetic manipulations to reduce overall protamine levels cause defective spermatid nuclear shaping and condensation (Cho et al., 2001). Transition proteins (Tnp) are intermediates in the histone–protamine transition, and recent gene knockout studies suggest overlapping functions for the two Tnp proteins, Tnp1 and

* Corresponding authors. Department of Biological Chemistry, College of Medicine, University of California, Irvine, CA 92697-1700, USA. Fax: +1 949 824 2688.
E-mail address: xdai@uci.edu (X. Dai).
[1] These authors have contributed equally to this work.

0012-1606/$ – see front matter © 2008 Elsevier Inc. All rights reserved.
doi:10.1016/j.ydbio.2008.05.553

Tnp2, in chromatin condensation and sperm development (Meistrich et al., 2003; Shirley et al., 2004; Zhao et al., 2004).

The chromatin incorporation of histone variants and the hyperacetylation of histones have been proposed to underlie the process of histone replacement during spermiogenesis (Govin et al., 2004). The histone variant H1FNT is expressed in developing spermatids and is important for proper DNA condensation during spermatid elongation (Martianov et al., 2005; Tanaka et al., 2005). H1fnt mutant male mice are characterized by delayed germ cell nuclear condensation, aberrant elongation of spermatids, and greatly reduced fertility. It is generally believed that histone hyperacetylation weakens the histone–DNA interaction, thereby creating a more open chromatin structure. The observation that histone H4 becomes hyperacetylated immediately before the histone-to-protamine transition has led to the proposal that H4 hyperacetylation facilitates histone displacement (Grimes and Henderson, 1984b; Meistrich et al., 1992). Although hyperacetylation of additional histones such as H3 has been found to co-exist with H4 hyperacetylation (Grimes and Henderson, 1984a; Hazzouri et al., 2000), less attention has been given to the potential involvement of these histone modifications in germ cell chromatin remodeling.

Here we show that Pygo2 is expressed in elongating spermatids and that mice containing hypomorphic alleles of *Pygo2* are infertile with drastic spermiogenic defects and reduced expression of Prm1, Prm2, Tnp2 and H1fnt. Furthermore, we provide evidence that Pygo2 in the testis associates with a histone acetyltransferase (HAT) activity, and a reduction in *Pygo2* expression levels leads to a specific decrease in lysine (K) 9/14 acetylation of histone H3. Finally, we show that although Wnt/β-catenin signaling is active in differentiating germ cells, the function of Pygo2 in spermiogenesis is not linked to nuclear β-catenin.

Materials and methods

Mouse breeding

Mice used for analysis were maintained in a 129Sv (129)×C57BL/6 (B6) mixed (50:50) genetic background. Genotyping was performed as previously described, with Southern blot analysis of DNAs isolated from *f/f Pygo2* mice showing no evidence of gene duplication or deletion (Li et al., 2007).

Histology, immunofluorescence and immunohistochemistry

Whole testes, epididymis, and vas deference from male mice were fixed overnight in Bouin's fixative or 4% paraformaldehyde, processed and embedded in paraffin wax or OCT. Sections (6–8 μm) were stained with periodic acid/Schiff sulfite leucofuchsin (PAS) or hematoxylin/esosin, DAPI, or the appropriate antibodies. Immunofluorescence was performed as described (Nair et al., 2006). The following antibodies were used: rabbit polyclonal α-Pygo2 antibody (Li et al., 2007), rabbit α-LDHC4 antibody (Hintz and Goldberg, 1977), mouse monoclonal α-β-catenin antibody (Sigma, Cat # C7207), α-acetyl-K9/14-histone H3 antibody (Upstate, Cat # 06-599), α-acetyl-K9-histone H3 antibody (Genetex, Cat # GTX12179), α-acetyl-K9/K14 histone H3 antibody (Upstate, Cat # 06-599), α-acetyl-K8-histone H4 and α-acetyl-K12-histone H4 antibodies (generous gifts from Michael Grunstein, UCLA), monoclonal α-trimethyl-K4-histone H3 antibody (Upstate, Cat # 05-745), and α-β-galactosidase antibody (MP Biomedicals, Cat # 55976). Immunohistochemistry was performed using a rat monoclonal IgM α-GCNA1 antibody (Enders and May, 1994) and the VECTASTAIN elite ABC kit (Vector) according to the manufacturer's suggestions.

Northern and RT-PCR

Total RNA was extracted from testis of 40-days old mice using Trizol (Invitrogen), and northern blot analysis performed using 35 μg of total RNA as described previously (Dai et al., 1998). A 374 bp fragment, generated by digesting the 3′ untranslated sequence of *Pygo2* (position 1927–2820 of the *Pygo2* cDNA; (Li et al., 2004)) with Pst I and Ear I, was used as a probe. For RT-PCR experiments, 5 μg of total RNA was reverse transcribed into cDNA using the Superscript III reverse transcriptase (Invitrogen). Sequences of primers used for PCR reactions are available upon request.

Seminiferous tubule squash preparation, germ cell and chromatin fractionation, and Western blot analysis

Whole testes from 40-day old mice was decapsulated in PBS. Stage-specific segments of seminiferous tubules were isolated using the transillumination-assisted microdissection technique (Kotaja et al., 2004). Squash preparations were performed as previously described (Kotaja et al., 2004). For germ cell fractionation, freshly dissected epididymis (including caput, corpus and cauda epididymis) from 3- to 4 testes of 40-day old mice were minced in 10 ml of ice-cold PBS, and kept at 4 °C for 15 min with constant agitation. The supernatant was filtered through a 74-mm mesh and centrifuged at 5000 ×*g* for 20 min. Pellets were washed once in 1 ml of ice-cold PBS and twice in 10 mM Tris–HCl, pH 8.0, 1 mM EDTA, which led to the lysis of contaminating blood and epithelial cells. Subsequently, centrifugal elutriation (Meistrich, 1977) was carried out to obtain enriched fractions of pachytene spermatocytes, round spermatids, and elongating/elongated spermatids. Purity was monitored and the number of resulting spermatozoa evaluated using a Nikon Diaphot TMD inverted microscope. Protein extraction and Western blotting were performed using standard procedures, and blots were probed with α-β-actin (Abcam, Cat # ab6276), α-Pygo2 (Li et al., 2007), and α-H1FNT (Martianov et al., 2005) antibodies. Chromatin fractionation was performed as previously described (Martianov et al., 2005). Briefly, whole testes were decapsulated in PBS and agitated on ice for 15 min after mincing. The cell mixture was transfer to 15 ml tubes and kept for 15 min, after which the supernatant was collected and centrifuged at 1000 ×*g* to remove tubular and Sertoli cells. The pellet, composed of mainly germ cells, was resuspended in N250 buffer (15 mM Tris, pH 7.5, 10 mM $MgCl_2$, 60 mM KCl, 15 mM NaCl, 1 mM $CaCl_2$, and 250 mM Sucrose) containing 0.3% NP40. After rocking for 15 min, the mixture was centrifuged at 2000 ×*g*, and the supernatant collected as the cytoplasmic fraction. The pellet was washed by N250 buffer three times and resuspended in PIPES (10 mM PIPES and 10 mM EDTA, pH 8.0) buffer. The resulting mixture was centrifuged at 6000 ×*g*, and the supernatant collected as the nucleoplasmic fraction and the pellet as the chromatin fraction. Throughout the procedure, the *f/f* samples were resuspended in smaller volumes than the wild-type to ensure comparable cell/volume ratios.

Co-immunoprecipitation (Co-IP) and histone acetyltransferase (HAT) activity assay

Co-IP of whole testis extracts prepared from 40-day old mice was carried out in 20 mM HEPES pH 7.9, 1 mM EDTA, 1 mM EGTA, 150 mM NaCl, 10% glycerol, 1 mM DTT, 1 mM Na_3VO4, plus protease inhibitors, using rabbit polyclonal α-Pygo2 antibody (Li et al., 2007) or control normal rabbit IgG (Santa Cruz Biotechnology, Santa Cruz, CA). Following overnight incubation at 4 °C, immuno-complexes were collected with Protein A/G beads, washed 4 times, eluted by boiling in 2× sample buffer, and subjected to SDS-PAGE and Western blotting with biotinylated α-Pygo2 (R&D systems, Minneapolis, MN), or α-β-catenin (Sigma, St. Louis, MO). HAT assay was performed according to manufacturer's instructions (Upstate, Cat # 17-289). Briefly, streptavidin-coated strip plates were incubated with biotinylated histone H3 or H4 peptides. Immunoprecipitates were then added in appropriate buffers, and strip plates washed and probed for acetylation of the histone peptides using an α-acetyl-lysine antibody. Acetylated histone H3 or H4 peptides were used as positive controls for antibody reaction and colorimetric analysis.

Results

Pygo2 is expressed in elongating/condensing spermatids and associates with the chromatin

In order to study the expression profile of Pygo2 in male germ cells, an α-Pygo2 antibody (Li et al., 2007) that specifically recognizes an expected 50 kDa protein in testicular extracts (Supplemental Figs. 1 and 2) was used to immunostain frozen testis sections and squash preparations of stage-specific segments of seminiferous tubules. A systematic analysis of seminiferous stage-specific germ cells revealed a strong presence of Pygo2 protein in spermatids from step 8 to step 12, encompassing those that undergo elongation and subsequently nuclear condensation (Fig. 1). The Pygo2 protein was found to be nuclear in step 8–9 spermatids (Figs. 1B, E, H), but as elongation proceeds it became localized to what appears to be acrosome at the anterior dorsal aspect of step 10 spermatids (Fig. 1K). In step 12 spermatids, the protein is predominantly present at the nuclear periphery of the sperm head (Fig. 1N). Biochemical fractionation experiments revealed the presence of Pygo2 protein in both nuclear and cytoplasmic fractions of purified elongating/elongated spermatids, and demonstrated that in the nucleus, the protein is predominantly chromatin-associated (Fig. 1O).

Nuclear Pygo2 was also detected in A-type spermatogonia, Sertoli cells, Leydig cells, and peritubular myoid cells (Fig. 1A, Supplemental Fig. 2). Consistently, the *Pygo2* transcripts were detected in testis of 1 week-old males, where only spermatogonia and somatic cell types were present (Supplemental Fig. 2G). Weak to no signal was

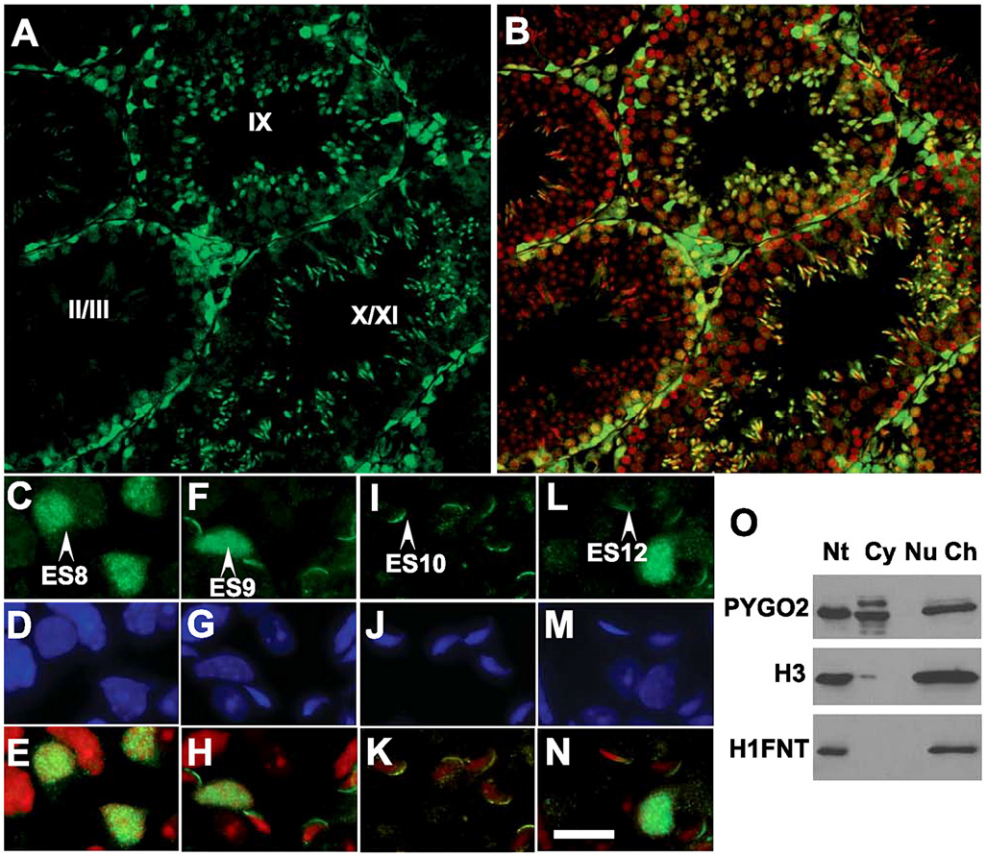

Fig. 1. Pygo2 protein is detected in elongating spermatids between steps 8–12. (A) Results of immunostaining of a testis section containing seminiferous tubules of different stages. Note Pygo2 expression in spermatids of step 9 (stage IX), step 10/11 (stage X/XI), but not in round spermatids or step 14 maturing spermatozoa (stage II/III). Panel B is a merged image of Pygo2 (green) and DAPI (artificially colored red) staining. (C–N) Squash preparations containing step 8 (C–E), 9 (F–H), 10 (I–K), and 12 (L–N) spermatids immunostained with anti-Pygo2 antibody. Arrowheads point to spermatids of step 8 (ES8), 9 (ES9), 10 (ES10), and 12 (ES12). Panels D, G, J, M are corresponding DAPI images of panels C, F, I, L, respectively. Panels E, H, K, and N are merged images with DAPI artificially colored red. (O) Nuclear Pygo2 associates with the chromatin. Nt, total nuclear fraction; Cy, cytoplasmic fraction; Nu, nucleoplasmic fraction; Ch, chromatin fraction. Histone H3 and H1FNT proteins serve as positive controls for chromatin fractionation. Scale bar: 60 μm in panels A, B; 6 μm in panels C–N.

detected in spermatocytes and round spermatids (Fig. 1 and data not shown). These results raised the possibility that *Pygo2* plays a role in male germ cell differentiation, especially during spermiogenesis.

Reduced levels of Pygo2 results in male infertility

We previously generated both null and conditional *floxed* (*f*) alleles of *Pygo2* and showed that germline deletion of *Pygo2* results in death shortly after birth (Li et al., 2007). Analysis of testes from E18.5 wild-type and null embryos revealed no apparent difference (data not shown), suggesting that embryonic germ cell development is normal in the absence of *Pygo2*. Interestingly, mice homozygous for the *f* allele of *Pygo2* (Li et al., 2007) survived to adulthood but showed male-specific sterility, offering a potential model to explore *Pygo2* function in postnatal testis. *f/f* males displayed normal mating behavior but multiple breedings yielded no offspring. Results of northern and Western blot analyses showed reduced levels of the 3.2-kb *Pygo2* transcript (2.2±0.3-fold) and 50-kD Pygo2 protein (2.4 ±0.5-fold) in *f/f* testis (Figs. 2A, B), suggesting that the presence of loxP sites in introns flanking exon 3 of *Pygo2* (Li et al., 2007) results in a hypomorphic allele. The reduction of Pygo2 levels in spermatids was confirmed by immunofluorescence of frozen testis sections (data not shown). Interestingly, the nuclear/cytoplasmic distribution of Pygo2 was abnormal in *f/f* testis, as there was a disproportional decrease in Pygo2 levels in the nucleus (Fig. 2C). Although *f/f* mice displayed no visible morphological defects in somatic tissues (data not shown), a reduction in *Pygo2* transcript levels was also observed for several somatic tissues in *f/f* mice when compared with wild-type controls (Supplemental Fig. 3), further supporting the notion that the *floxed* allele of *Pygo2* is hypomorphic. In contrast to *f/f* males, *+/f* and +/null heterozygous males are fertile. Together, these data suggest that reduced Pygo2 levels in *f/f* mice associate with male infertility.

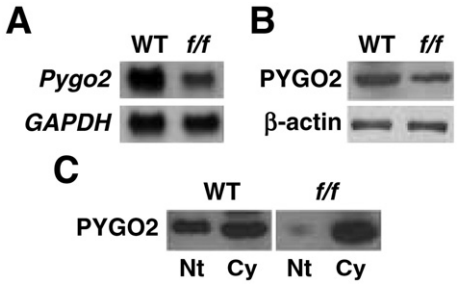

Fig. 2. Reduced *Pygo2* expression in *f/f* testis. (A) Results of northern blot analysis of RNAs isolated from wild-type and *f/f* testes. A single *Pygo2* transcript of 3.2 kb was detected in both wild-type and mutant samples. (B) Results of Western blot analysis of testicular extracts prepared from wild-type and *f/f* testes. Note reduced levels of the 50-kDa Pygo2 protein in mutant samples. *GAPDH* transcripts and β-actin proteins were used as loading controls. The *Pygo2*/Pygo2 band intensities were quantified by densitometer tracing and fold reduction was determined from multiple experiments after normalization against band intensities of loading controls. (C) The *f/f* mutation preferentially impacts nuclear Pygo2 levels.

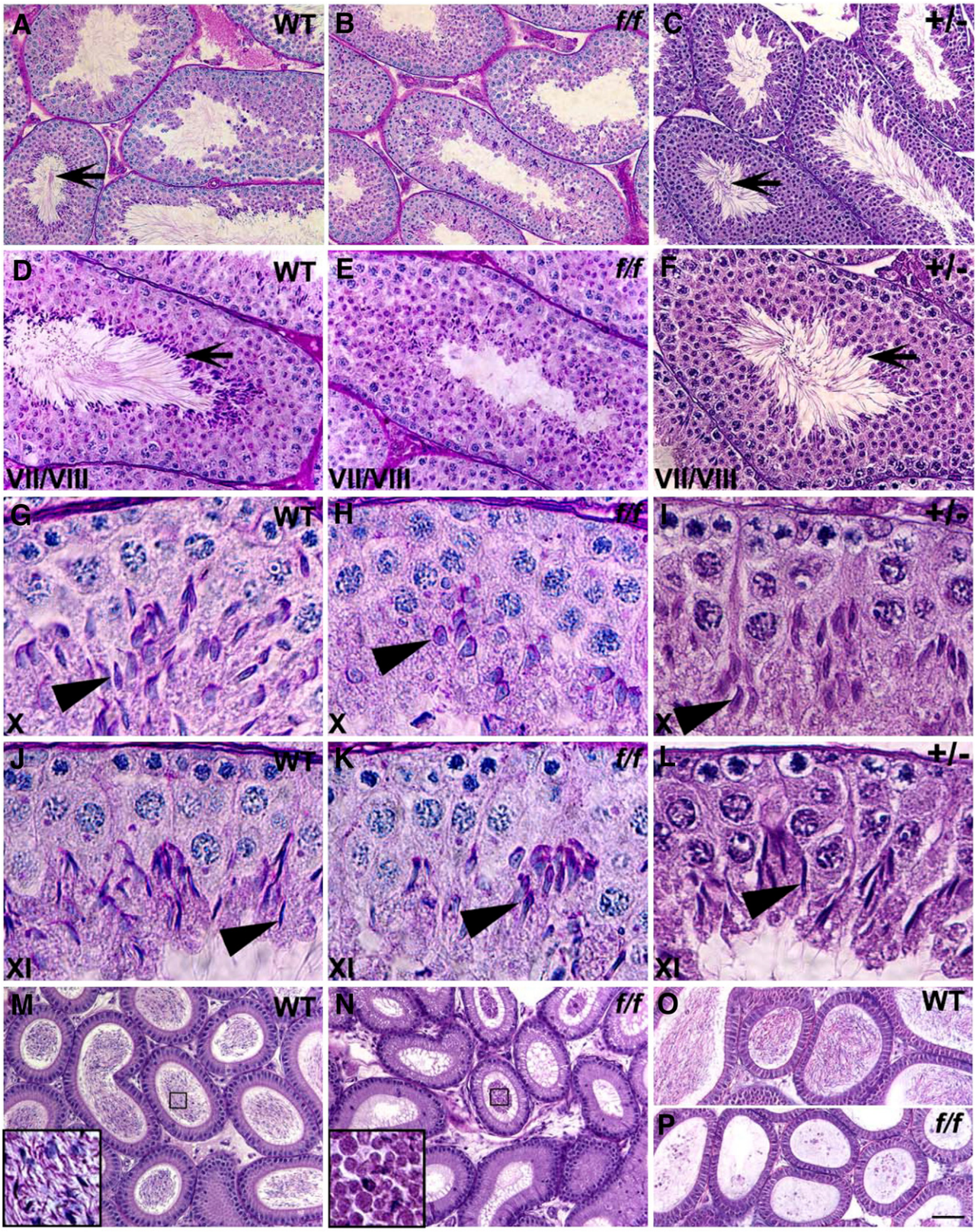

Fig. 3. Defective spermiogenesis in *f/f* mice. (A–C) Histological analysis of testis sections from adult wild-type (WT) (A), *f/f* (B) and +/− (C) males. Arrows indicate the elongated spermatids or spermatozoa that are present in the seminiferous tubules of wild-type and +/− testes but absent in *f/f* littermates. (D–F) Morphology of stage VII–VIII seminiferous tubules from wild-type (D), *f/f* (E), and +/− (F) males. Arrowheads indicate the normal elongated spermatids in wild-type and +/− mice; such cells are completely absent in *f/f* littermates. (G–I) Morphology of stage X seminiferous tubules from wild-type (G), *f/f* (H), and +/− males. Note that the normal nuclear elongation of wild-type and +/− step 10 spermatids (arrowheads) is not observed in the *f/f* counterparts. (J–L) Morphology of stage XI seminiferous tubules from wild-type (J), *f/f* (K), and +/− (L) males. Note the improper nuclear condensation of step 11 spermatids (arrowheads) in the *f/f* mutant. (M–P) Morphology of wild-type (M, O) and *f/f* (N, P) epididymis (M, N) and vas deferens (O, P). Insets in panels M and N show enlarged images of the boxes areas. Scale bar: 60 μm in panels A–C,M–P; 30 μm in panels D–F; 10 μm in panels G–L.

Defective spermiogenesis in f/f Pygo2 males

At a histological level, the most striking defect in adult mutant testis was the lack of elongated spermatids (Fig. 3B). Analysis of stage-matched seminiferous tubules from juvenile wild-type and *f/f* mice demonstrated that in the mutant the cellular associations normally observed in wild-type testis were disrupted, that round, elongating, and elongated spermatids sometimes co-exist in a single tubule indicative of asynchronous spermatid development, and that step 16 spermatids were completely absent (Fig. 3E). The earliest morphological defects were detected in step 9–10 spermatids, coinciding with the stages when Pygo2 expression in haploid germ cells became prominent and is primarily nuclear. However, the total number of elongating spermatids was maintained in the *f/f* tubules (53% of total germ cells in stage X/XI *f/f* tubules are step 10 and 11 spermatids, as compared to 54% in the wild-type). Comparing to their wild-type counterparts, step 10 spermatids in the mutant did not properly elongate their nuclei (Fig. 3H), and the nuclei of step 11 mutant spermatids were not properly condensed (Fig. 3K). These results highlight defective nuclear elongation and condensation as the primary defects in *f/f* testis. In contrast to *f/f* mice, heterozygous (+/−) males showed no detectable spermiogenic defects (Figs. 3C, F, I, L). Examination of the histology of epididymis and vas deferens revealed that while wild-type and +/− epididymis and vas deferens contained abundant mature spermatozoa (Figs. 3M, O and data not shown), few spermatozoa were observed in the *f/f* mutant littermates (Figs. 3N, P). The occasionally seen spermatozoa displayed round heads with no tails (Fig. 3N inset), confirming a failure in nuclear shaping.

At a biochemical level, expression of LDHC4, a marker for germ cells from mid/late-pachytene stage onward (Hintz and Goldberg, 1977), was not affected (Figs. 4A, B). Furthermore, expression of GCNA1 (germ cell nuclear antigen), a marker for spermatogonia and spermatocytes prior to mid-pachytene (Enders and May, 1994), was largely normal, and there is no reduction in the number of GCNA1-positive cells in the mutant (Figs. 4C, D). These results suggest that the *f/f* mutation does not significantly impact the early steps of spermatogenesis.

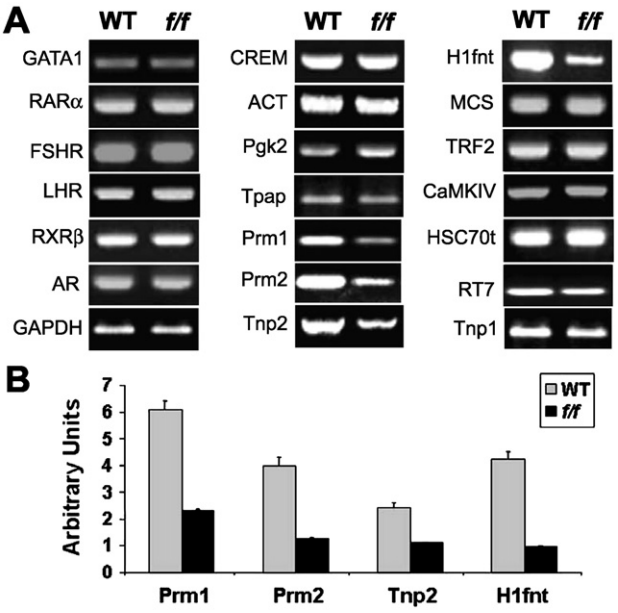

Fig. 5. Select reduction of haploid gene expression in *f/f* spermatids. Shown are results of semi-quantitative (A) and real-time (B) PCR analysis revealing decreased mRNA levels of Prm1, Prm2, Tnp2, and H1fnt but not other genes. Real-time PCR data represent average of four different mice, each assayed in triplicates.

Decreased expression of select post-meiotic genes in f/f testis

To explore the molecular defects of *Pygo2*-reduced germ cells, we performed RT-PCR analysis to examine the expression of regulatory

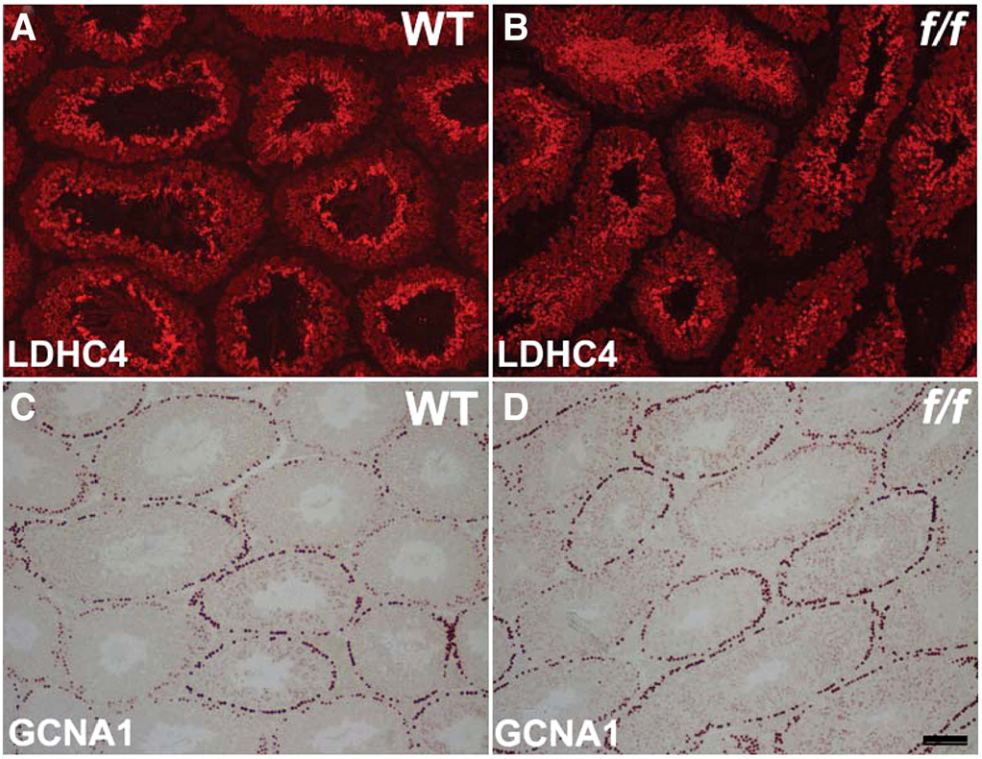

Fig. 4. Biochemistry of wild-type and *f/f* testes. Shown are results of immunofluorescence staining using anti-LDHC4 antibody (A, B) and immunohistochemical analysis using anti-GCNA1 antibody (C, D) on wild-type (A, C) and *f/f* (B, D) testes. Scale bar: 80 μm.

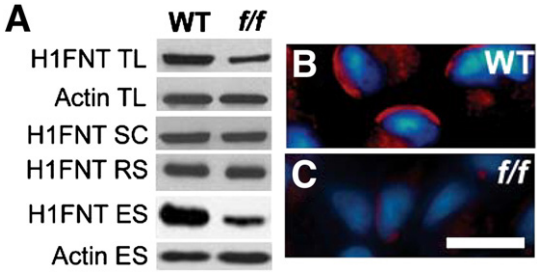

Fig. 6. H1FNT protein levels are reduced in elongating/elongated *f/f* spermatids. (A) Western blot analysis showing reduced H1FNT protein levels in total testis lysates (TL) and elongating/elongated spermatids (ES), but not in spermatocytes (SC) and round spermatids (RS). Actin was used as a loading control. (B, C) The polarized H1FNT protein localization (red) in wild-type spermatids (B) is greatly diminished in the *f/f* (C) counterparts. Blue, DAPI staining to visualize nuclei. Scale bar: 6 μm.

and structural genes that have been implicated in spermatogenesis. Genes that are normally expressed in Sertoli cells, including GATA1, RARα, and FSHR (Heckert and Griswold, 1991; Kliesch et al., 1992; Vernet et al., 2006; Yomogida et al., 1994), showed unaltered expression in *f/f* testis (Fig. 5A). Similarly, genes the expression of which is Leydig cell-specific or -enriched, including LHR and RXRβ (Gaemers et al., 1998; Zhang et al., 1994), were not affected. AR has been reported to be expressed in both somatic (Sertoli, Leydig, peritubular myoid cells) and germ cells (Vornberger et al., 1994), and no change was seen in *f/f* testis. These results suggest that the *f/f* mutation of *Pygo2* may not impact the somatic Sertoli and Leydig cells.

Germ cell-expressing genes were differentially affected. Those with a reported expression in round spermatids and earlier, such as CREM (Delmas et al., 1993), ACT (Fimia et al., 1999), Pgk2 (Gold et al., 1983), Tpap (Kashiwabara et al., 2000), produced normal levels of mRNAs in *f/f* testis. In contrast, there was a dramatic reduction of mRNA levels of several genes with expression normally activated in late round spermatids and high in elongating spermatids (Mali et al., 1989; Saunders et al., 1992), including Prm1 (decreased by 2.6-fold), Prm2 (decreased by 3.4-fold), Tnp2 (decreased by 2.1-fold), and H1fnt (decreased by 4.3-fold), in *f/f* testis (Figs. 5A, B). However, this reduction is not universal for all late-spermatid-expressing genes, as MCS (Nam et al., 1997), TRF2/TLF (Martianov et al., 2001), CaMKIV (Wu and Means, 2000), HSC70t (Tsunekawa et al., 1999), and RT7/ODF (Morales et al., 1994; van der Hoorn et al., 1990) were all expressed at apparently normal levels. Importantly, Tnp1 is normally expressed in a pattern reminiscent of those of Prm1, Prm2, and Tnp2 (Mali et al., 1989), yet its expression level was only minimally affected in *f/f* testis.

We next performed proof-of-principle experiments to see if the altered mRNA levels observed above indeed translate into altered protein levels. A significant reduction in H1FNT protein levels was

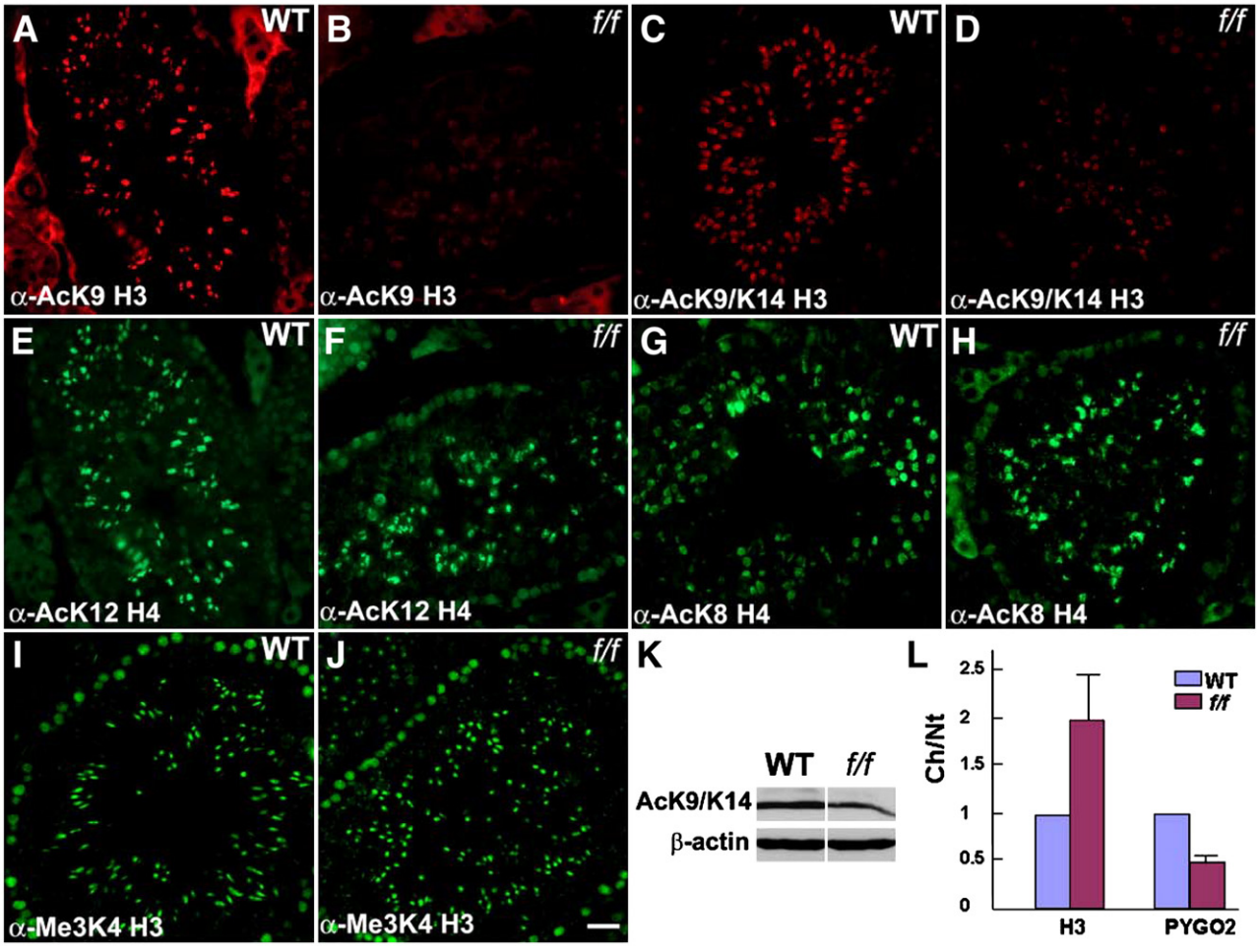

Fig. 7. Hyperacetylation at K9/K14 of histone H3 is specifically reduced in elongating *f/f* spermatids. (A, B, E, F) Results of double-immunostaining of wild-type (A, E) and *f/f* (B, F) testes using anti-acetyl-K9 H3 (A, B) and anti-acetyl-K12 H4 (E, F) antibodies. Shown are stage IX seminiferous tubules. Note reduced histone H3 K9 acetylation in stage 9 spermatids. (C, D, G–J) Results of immunostaining of wild-type (C, G, I) and *f/f* (D, H, J) testes using anti-acetyl-K9/K14 H3 (C, D), anti-acetyl-K8 H4 (G, H) or anti-trimethyl-K4 H3 (I, J) antibodies. (K) Western blot analysis of lysates prepared from fractionated elongating/elongated spermatids. (L) Plot of chromatin/nuclear (Ch/Nt) ratios for histone H3 and Pygo2. Western blot signals of chromatin or total nuclear fractions were quantified from two independent experiments and average values are shown. Scale bar: 30 μm.

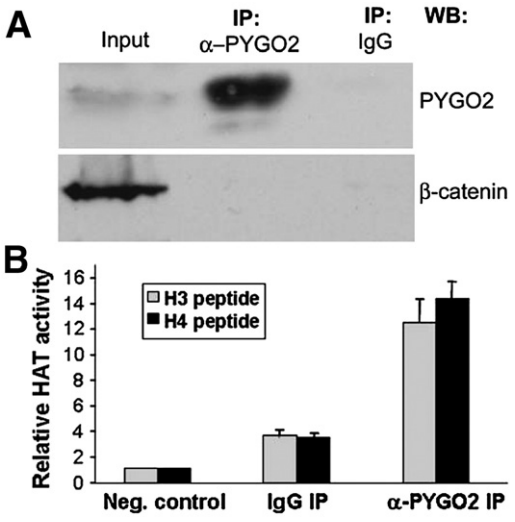

Fig. 8. Pygo2 associates with HAT in testis. (A) Western blotting analysis showing absence of β-catenin in anti-Pygo2 immunoprecipitates. (B) HAT activity is detected in anti-Pygo2 immunoprecipitates. Values obtained without the presence of any substrate (negative control) were arbitrarily set as 1.

observed in *f/f* testis lysates, as well as in lysates prepared from isolated preparations of *f/f* elongating/elongated spermatids (Fig. 6A). In contrast, no decrease occurred in *f/f* spermatocytes or round spermatids. Immunofluorescence analysis of squash preparations demonstrated the characteristic H1FNT localization to the dorsal anterior aspect of nuclei of wild-type elongating spermatids, whereas mutant spermatids almost lacked this expression (Figs. 6B, C). H1FNT is known to tightly associate with the chromatin (Martianov et al., 2005), but this chromatin association was not affected in *f/f* testis (data not shown). Collectively, the results in this section suggest a specific role for Pygo2 in controlling the expression of select late-spermatid genes including protamines, Tnp2, and H1fnt.

Pygo2 is required for histone H3 hyperacetylation in elongating spermatids and associates with a HAT activity

PHD finger proteins have been implicated in the recognition of K4-trimethylated histone H3 and facilitate subsequent H3 acetylation (Li et al., 2006; Pena et al., 2006; Shi et al., 2006; Taverna et al., 2006; Wysocka et al., 2006). Since Pygo2 contains an evolutionarily conserved PHD finger, we wondered whether it too may play a facilitating role in germ cell histone acetylation. Double staining of the same testis sections using anti-acetyl-K9 of histone H3 (AcK9 H3) and anti-acetyl-K12 of histone H4 (AcK12 H4) revealed identical patterns in elongating spermatids of wild-type mice (Figs. 7A, E), suggesting that histone H3 K9 acetylation occurs concomitantly with H4 hyperacetylation during spermatid development. While no difference was detected between wild-type and *f/f* males in K12 or K8 acetylation of histone H4 (AcK12 H4 or AcK8 H4) (Figs. 7E–H), we observed a significant reduction in the extent of K9 acetylation of histone H3 in *f/f* spermatids (Fig. 7B). A similar reduction in staining intensity was observed when an antibody that recognizes both acetyl-K9 and acetyl-K14 of histone H3 (AcK9/K14 H3) was used (Fig. 7D). Reduced histone H3 acetylation was obvious in stage 9 spermatids (Figs. 7B, D), where Pygo2 protein is predominantly nuclear, and persisted until later stages (data not shown). In contrast to acetylation, immunofluorescence analysis failed to reveal any significant change in the levels of K4-trimethylated histone H3 (Me3K4 H3) in *f/f* germ cells (Fig. 7J).

To quantitatively assess the changes in histone H3 acetylation, we performed Western blot analysis of lysates prepared from purified elongating/elongated spermatids. Comparing to the wild-type, a ~2-fold reduction in K9/K14-acetylated histone H3 levels was seen in *f/f* elongating/elongated spermatids (Fig. 7K). To evaluate the possible significance of reduced histone H3 acetylation, we assessed the chromatin-bound fraction of histone H3 in wild-type and *f/f* testes by determining the apparent chromatin/total nuclear ratio of the protein. Relative to wild-type samples, a higher proportion of histone H3 was chromatin-bound in *f/f* testes (Fig. 7L). In contrast, the chromatin/nuclear ratio was decreased in *f/f* samples for Pygo2. Taken

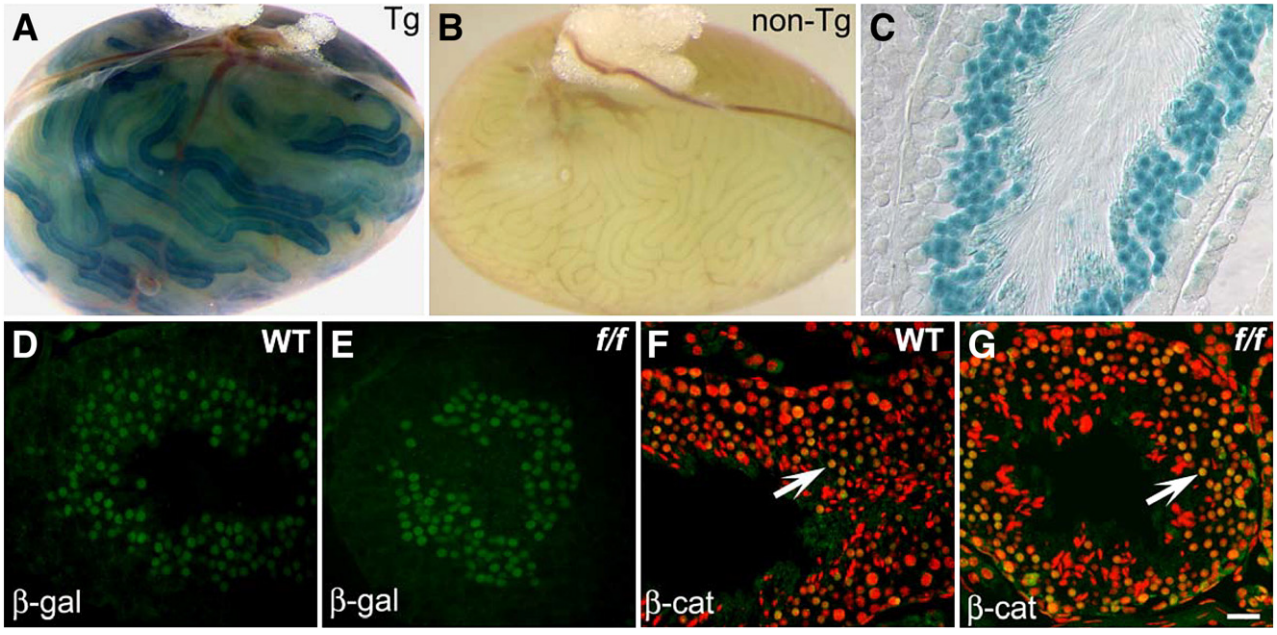

Fig. 9. Spermatids from *f/f* mice show largely normal LEF/TCF-responsive promoter activity and β-catenin nuclear localization. (A, B) Whole-mount staining for β-galactosidase activity of testes from BAT-gal transgenic (Tg) (A) and non-transgenic (non-Tg) littermates (B). A section of the Tg testis is shown in panel C. (D, E) Immunostaining using anti-β-galactosidase antibody of testis sections from wild-type (D) and *f/f* (E) mice that carry the BAT-gal transgene. (F, G) Immunostaining of wild-type (F) and *f/f* (G) testes using anti-β-catenin antibody. DAPI staining of the sections was artificially colored red and superimposed with anti-β-catenin staining to illustrate the nuclear location of the β-catenin protein in round spermatids (white arrows). Scale bar: 18 μm in panel C; 15 μm in panels D–G.

together, these results identify Pygo2 as a regulator of global histone H3 hyperacetylation in elongating spermatids, and correlate mis-regulated acetylation with aberrant chromatin retention of histone H3 in Pygo2-reduced testis.

We next asked whether Pygo2, like PHD finger protein Yng1 (Taverna et al., 2006), associates with a HAT activity. Extracts from mouse testis were used for immunoprecipitation using anti-Pygo2 antibody, and it was evident that the antibody precipitated the endogenous Pygo2 protein (Fig. 8A). When HAT activity was measured, a significant enrichment of an activity that was able to acetylate both histone H3 and H4 peptide substrates was observed in α-Pygo2 immunoprecipitates over IgG controls (Fig. 8B). Interestingly, β-catenin was not detected in the immunoprecipitates. As a control, we note that Pygo2-β-catenin interaction was detected in 293T cells in our hands (data not shown). Collectively, our results demonstrate that Pygo2 in testis associates with a HAT activity likely in a β-catenin-independent manner, providing a possible biochemical mechanism for Pygo2's regulation of histone acetylation in germ cells.

In vivo evidence that Pygo2 and β-catenin have independent regulatory pathways in male germ cells

Next we performed experiments to directly address whether Pygo2 functions in spermiogenesis by regulating the transcriptional output of Wnt/β-catenin signaling. We first examined the expression of BAT-gal, a widely used Wnt reporter gene in which LacZ expression is under the control of LEF/TCF-responsive elements (Maretto et al., 2003), in testis. Testes from BAT-gal transgenic mice stained blue with β-galactosidase substrates (Fig. 9A), while non-transgenic littermates appeared white (Fig. 9B). The predominant sites of LacZ expression were round spermatids (Figs. 9C, D). The β-galactosidase protein persisted in early elongating (step 9–10) spermatids but diminished upon further maturation (data not shown). These results imply the presence of factors in round spermatids that can activate LEF/TCF target gene expression. Indeed, nuclear β-catenin, presumably produced as a result of active Wnt signaling, was detected in round spermatids (Fig. 9F) and weakly in pachytene spermatocytes, but not in elongating spermatids that normally express Pygo2 (data not shown). No significant reduction in β-galactosidase activity or expression was observed in round and early elongating spermatids of *f/f* mice (Fig. 9E and data not shown), indicating that reduced Pygo2 levels have little effect on the activity of the LEF/TCF-responsive promoter that is present in the BAT-gal transgene. Furthermore, nuclear localization of β-catenin was still detected in *f/f* round spermatids (Fig. 9G). These results, together with the biochemical data above showing that β-catenin and Pygo2 in testis do not co-immunoprecipitate, suggest that the actions of β-catenin and Pygo2 are spatially separated, and that Pygo2 function in spermiogenesis is β-catenin-independent.

Discussion

Spermiogenesis entails a major biochemical and morphological restructuring of the germ cell involving replacement of somatic histones by protamines packing the DNA into the condensed spermatid nucleus during the elongation phase. Our results uncover an important role for Pygo2 in mammalian spermiogenesis, as reduced levels of Pygo2 originated from hypomorphic *floxed* alleles result in a complete spermiogenic arrest and male infertility. Pygo2-reduced spermatids fail to properly elongate and shape their nuclei, and these phenotypes partially overlap those observed in mouse mutants of protamines, transition proteins, and H1fnt. Indeed, we observed a decreased expression of Prm1, Prm2, Tnp2, and H1fnt in *f/f* testis. This effect is rather specific, as other late-spermatid-expressing genes such as Tnp1 are not affected. Therefore, it is unlikely that the reduced expression of H1fnt, Prm1, Prm2, and Tnp2 is simply due to a reduced presence of late spermatids in *f/f* testis. In mice and humans, genes encoding Prm1, Prm2, and Tnp2 are clustered together on one chromosome and their expression coordinately regulated in a haploid-specific manner during spermatogenesis (Nelson and Krawetz, 1993), whereas the Tnp1 gene is located on another chromosome. The uniform down-regulation of the clustered genes in *f/f* testis raises an intriguing possibility that Pygo2 directly or indirectly regulates the activation of this gene cluster in a concerted manner. This notion is worth testing experimentally. Prm1, Prm2, Tnp1, and RT7 are all downstream targets of CREM, a key haploid germ cell transcription factor (Delmas et al., 1993). The largely unaltered expression of Tnp1 and RT7 also suggests that Pygo2 reduction does not result in a general decrease in CREM-dependent transcription.

Besides a potential role in regulating specific haploid genes, a functional Pygo2 protein is essential in vivo for K9/K14 hyperacetylation of histone H3. We show that H3 hyperacetylation occurs during spermatid elongation and nuclear condensation, and that it is selectively reduced in *f/f* mutant spermatids. While it is formally possible that this defect is a secondary consequence of other cellular/molecular changes such as those that may occur in the somatic support cells or in premeiotic germ cells, two pieces of evidence are consistent with a more direct role for Pygo2 in the acetylation of histone H3: 1) histone H3 hyperacetylation and its decrease in *f/f* mutant spatiotemporally correlate with abundant nuclear expression of Pygo2; 2) Pygo2 associates with a HAT activity in testis extracts. One of the proposed consequences of histone hyperacetylation is the facilitated displacement of histones from the chromatin. Consistently with this hypothesis, we observed an increased chromatin association (retention) of histone H3 in *f/f* mutant testis. Our results offer no insights as to the relative importance of Pygo2's effect on haploid gene expression and histone H3 acetylation. Our current thinking is that Pygo2 regulates both events in elongating spermatids, thereby coordinating histone displacement with the production of proteins that can take histones' place to package the germ cell DNA in a more compact fashion.

Which HAT does Pygo2 associate with? Our results of HAT assays on purified histone peptide substrates indicate that this HAT does not distinguish between H3 and H4 in vitro. Therefore, it is unlikely that the Pygo2-associated HAT is CDYL, which has been previously identified as a histone H4-specific HAT expressed in maturing spermatids (Lahn et al., 2002). Despite the in vitro promiscuity of Pygo2-associated HAT, reduced Pygo2 levels affect histone H3 but not H4 hyperacetylation. This in vivo specificity implicates the existence of additional mechanisms that target Pygo2-associated activity to histone H3. PHD fingers have recently been found to be a recognition motif for histone H3 trimethylated at K4 (Li et al., 2006; Pena et al., 2006; Shi et al., 2006; Wysocka et al., 2006). Furthermore, K4 trimethylation of histone H3 facilitates its subsequent acetylation by Yng1-associated HAT (Taverna et al., 2006). Global K4 trimethylation of H3 during germ cell development has recently been shown to spatiotemporally overlap global histone hyperacetylation (Godmann et al., 2007), but the underlying molecular link between these two modification events is unclear. We propose that the PHD domain of Pygo2 binds to K4-trimethyl histone H3 in germ cell chromatin, thereby targeting Pygo2-associated HAT activity to histone H3. Clearly, future studies beyond the scope of this work are needed to test our model and to identify the Pygo2-associated HAT.

Testes of *f/f* mice express Pygo2 at a level that is approximately 40% of the wild type. Since +/null heterozygous – presumably expressing 50% of wild-type level of Pygo2 – and *+/f* males are fertile with no apparent defects in spermatid elongation, we surmise that there is a critical threshold of Pygo2 dosage below which spermiogenesis cannot be sustained. We note the interesting finding that the nuclear concentration of Pygo2 appears to be disproportionally impacted by the mutation comparing to the cytoplasmic concentration. Perhaps a

threshold level of Pygo2 is necessary for efficient nuclear localization; when Pygo2 levels drop below this threshold, the cytoplasmic/nuclear distribution is altered, leading to a specific reduction in protein levels inside the nucleus. Dissecting the underling mechanism of this observation is outside the scope of the current work. Alternatively, the *f/f* mutation may have an allele-specific effect. *f/f* mice do not display apparent defects in somatic epithelial tissues that are known to be affected by a *Pygo2* null mutation (Li et al., 2007). This difference reveals a tissue- and cell type-specific sensitivity of developmental processes to Pygo2 protein levels. Remodeling of the germ cell chromatin during spermatid elongation is global in nature, whereas chromatin remodeling in somatic cells is more gene- and locus-specific. Therefore, elongating spermatids may entail a higher level of nuclear Pygo2 proteins for proper chromatin modifications, and are therefore particularly sensitive to the *f/f*-induced reduction in Pygo2 levels.

Our data demonstrate that canonical Wnt signaling is active (by virtue of expressing nuclear β-catenin and activating a LEF/TCF target promoter) in differentiating germ cells, particularly in spermatocytes and round spermatids. However, this activation does not seem to require Pygo2, as Pygo2 protein is not detected in these cells. Instead, Pygo2 is present in elongating spermatids and is required for their further differentiation. Although we cannot fully exclude the possibility that there are subtle differences in Wnt signaling between wild type and mutant that are beyond our method of detection, our analysis supports the notion that the function of Pygo2 in male germ cells is independent of β-catenin, and by inference, Wnt signaling. This work is consistent with previous reports to show that mammalian *Pygopus* genes have evolved to perform Wnt-independent functions in addition to their roles in mediating canonical Wnt signaling (Li et al., 2007; Schwab et al., 2007; Song et al., 2007).

Acknowledgments

We thank Wen-Hwa Lee for microscope use, Grant MacGregor for discussions, and anonymous reviewers for helpful suggestions. We are grateful to Erwin Goldberg and George Enders for kindly providing the α-LDHC4 and α-GCNA1 antibodies, respectively. This work was supported by a DOD grant W81XWH-04-1-0516, and NIH Grants R01-AR47320 and K02-AR51482 awarded to X. D.

Appendix A. Supplementary data

Supplementary data associated with this article can be found, in the online version, at doi:10.1016/j.ydbio.2008.05.553.

References

Balhorn, R., Reed, S., Tanphaichitr, N., 1988. Aberrant protamine 1/protamine 2 ratios in sperm of infertile human males. Experientia 44, 52–55.
Belenkaya, T.Y., Han, C., Standley, H.J., Lin, X., Houston, D.W., Heasman, J., 2002. pygopus Encodes a nuclear protein essential for wingless/Wnt signaling. Development 129, 4089–4101.
Chevaillier, P., Mauro, N., Feneux, D., Jouannet, P., David, G., 1987. Anomalous protein complement of sperm nuclei in some infertile men. Lancet 2, 806–807.
Cho, C., Willis, W.D., Goulding, E.H., Jung-Ha, H., Choi, Y.C., Hecht, N.B., Eddy, E.M., 2001. Haploinsufficiency of protamine-1 or -2 causes infertility in mice. Nat. Genet. 28, 82–86.
Clevers, H., 2006. Wnt/beta-catenin signaling in development and disease. Cell 127, 469–480.
Dai, X., Schonbaum, C., Degenstein, L., Bai, W., Mahowald, A., Fuchs, E., 1998. The ovo gene required for cuticle formation and oogenesis in flies is involved in hair formation and spermatogenesis in mice. Genes Dev. 12, 3452–3463.
de la Roche, M., Bienz, M., 2007. Wingless-independent association of Pygopus with dTCF target genes. Curr. Biol.
de Yebra, L., Ballesca, J.L., Vanrell, J.A., Bassas, L., Oliva, R., 1993. Complete selective absence of protamine P2 in humans. J. Biol. Chem. 268, 10553–10557.
Delmas, V., van der Hoorn, F., Mellstrom, B., Jegou, B., Sassone-Corsi, P., 1993. Induction of CREM activator proteins in spermatids: down-stream targets and implications for haploid germ cell differentiation. Mol. Endocrinol. 7, 1502–1514.
Enders, G.C., May II, J.J., 1994. Developmentally regulated expression of a mouse germ cell nuclear antigen examined from embryonic day 11 to adult in male and female mice. Dev. Biol. 163, 331–340.
Fimia, G.M., De Cesare, D., Sassone-Corsi, P., 1999. CBP-independent activation of CREM and CREB by the LIM-only protein ACT. Nature 398, 165–169.
Gaemers, I.C., van Pelt, A.M., van der Saag, P.T., Hoogerbrugge, J.W., Themmen, A.P., de Rooij, D.G., 1998. Differential expression pattern of retinoid X receptors in adult murine testicular cells implies varying roles for these receptors in spermatogenesis. Biol. Reprod. 58, 1351–1356.
Godmann, M., Auger, V., Ferraroni-Aguiar, V., Di Sauro, A., Sette, C., Behr, R., Kimmins, S., 2007. Dynamic regulation of histone H3 methylation at lysine 4 in mammalian spermatogenesis. Biol. Reprod.
Gold, B., Fujimoto, H., Kramer, J.M., Erickson, R.P., Hecht, N.B., 1983. Haploid accumulation and translational control of phosphoglycerate kinase-2 messenger RNA during mouse spermatogenesis. Dev. Biol. 98, 392–399.
Govin, J., Caron, C., Lestrat, C., Rousseaux, S., Khochbin, S., 2004. The role of histones in chromatin remodelling during mammalian spermiogenesis. Eur. J. Biochem. 271, 3459–3469.
Grimes Jr., S.R., Henderson, N., 1984a. Acetylation of rat testis histones H2B and TH2B. Dev. Biol. 101, 516–521.
Grimes Jr., S.R., Henderson, N., 1984b. Hyperacetylation of histone H4 in rat testis spermatids. Exp. Cell Res. 152, 91–97.
Hazzouri, M., Pivot-Pajot, C., Faure, A.K., Usson, Y., Pelletier, R., Sele, B., Khochbin, S., Rousseaux, S., 2000. Regulated hyperacetylation of core histones during mouse spermatogenesis: involvement of histone deacetylases. Eur. J. Cell Biol. 79, 950–960.
Heckert, L.L., Griswold, M.D., 1991. Expression of follicle-stimulating hormone receptor mRNA in rat testes and Sertoli cells. Mol. Endocrinol. 5, 670–677.
Hintz, M., Goldberg, E., 1977. Immunohistochemical localization of LDH-x during spermatogenesis in mouse testes. Dev. Biol. 57, 375–384.
Jessen, S., Gu, B., Dai, X. Pygopus and the Wnt signaling pathway a diverse set of connections. Bioessays, in press.
Kashiwabara, S., Zhuang, T., Yamagata, K., Noguchi, J., Fukamizu, A., Baba, T., 2000. Identification of a novel isoform of poly(A) polymerase, TPAP, specifically present in the cytoplasm of spermatogenic cells. Dev. Biol. 228, 106–115.
Kimmins, S., Sassone-Corsi, P., 2005. Chromatin remodelling and epigenetic features of germ cells. Nature 434, 583–589.
Kliesch, S., Penttila, T.L., Gromoll, J., Saunders, P.T., Nieschlag, E., Parvinen, M., 1992. FSH receptor mRNA is expressed stage-dependently during rat spermatogenesis. Mol. Cell Endocrinol. 84, R45–R49.
Kotaja, N., Kimmins, S., Brancorsini, S., Hentsch, D., Vonesch, J.L., Davidson, I., Parvinen, M., Sassone-Corsi, P., 2004. Preparation, isolation and characterization of stage-specific spermatogenic cells for cellular and molecular analysis. Nat. Methods 1, 249–254.
Kramps, T., Peter, O., Brunner, E., Nellen, D., Froesch, B., Chatterjee, S., Murone, M., Zullig, S., Basler, K., 2002. Wnt/wingless signaling requires BCL9/legless-mediated recruitment of pygopus to the nuclear beta-catenin–TCF complex. Cell 109, 47–60.
Krieghoff, E., Behrens, J., Mayr, B., 2006. Nucleo-cytoplasmic distribution of beta-catenin is regulated by retention. J. Cell Sci. 119, 1453–1463.
Lahn, B.T., Tang, Z.L., Zhou, J., Barndt, R.J., Parvinen, M., Allis, C.D., Page, D.C., 2002. Previously uncharacterized histone acetyltransferases implicated in mammalian spermatogenesis. Proc. Natl. Acad. Sci. U. S. A. 99, 8707–8712.
Li, B., Mackay, D.R., Ma, J., Dai, X., 2004. Cloning and developmental expression of mouse pygopus 2, a putative Wnt signaling component. Genomics 84, 398–405.
Li, H., Ilin, S., Wang, W., Duncan, E.M., Wysocka, J., Allis, C.D., Patel, D.J., 2006. Molecular basis for site-specific read-out of histone H3K4me3 by the BPTF PHD finger of NURF. Nature 442, 91–95.
Li, B., Rheaume, C., Teng, A., Bilanchone, V., Munguia, J.E., Hu, M., Jessen, S., Piccolo, S., Waterman, M.L., Dai, X., 2007. Developmental phenotypes and reduced Wnt signaling in mice deficient for pygopus 2. Genesis 45, 318–325.
Logan, C.Y., Nusse, R., 2004. The Wnt signaling pathway in development and disease. Annu. Rev. Cell. Dev. Biol. 20, 781–810.
Mali, P., Kaipia, A., Kangasniemi, M., Toppari, J., Sandberg, M., Hecht, N.B., Parvinen, M., 1989. Stage-specific expression of nucleoprotein mRNAs during rat and mouse spermiogenesis. Reprod. Fertil. Dev. 1, 369–382.
Maretto, S., Cordenonsi, M., Dupont, S., Braghetta, P., Broccoli, V., Hassan, A.B., Volpin, D., Bressan, G.M., Piccolo, S., 2003. Mapping Wnt/beta-catenin signaling during mouse development and in colorectal tumors. Proc. Natl. Acad. Sci. U. S. A. 100, 3299–3304.
Martianov, I., Brancorsini, S., Catena, R., Gansmuller, A., Kotaja, N., Parvinen, M., Sassone-Corsi, P., Davidson, I., 2005. Polar nuclear localization of H1T2, a histone H1 variant, required for spermatid elongation and DNA condensation during spermiogenesis. Proc. Natl. Acad. Sci. U. S. A. 102, 2808–2813.
Martianov, I., Fimia, G.M., Dierich, A., Parvinen, M., Sassone-Corsi, P., Davidson, I., 2001. Late arrest of spermiogenesis and germ cell apoptosis in mice lacking the TBP-like TLF/TRF2 gene. Mol. Cell 7, 509–515.
Meistrich, M.L., 1977. Separation of spermatogenic cells and nuclei from rodent testes. Methods Cell Biol. 15, 15–54.
Meistrich, M.L., Trostle-Weige, P.K., Lin, R., Bhatnagar, Y.M., Allis, C.D., 1992. Highly acetylated H4 is associated with histone displacement in rat spermatids. Mol. Reprod. Dev. 31, 170–181.
Meistrich, M.L., Mohapatra, B., Shirley, C.R., Zhao, M., 2003. Roles of transition nuclear proteins in spermiogenesis. Chromosoma 111, 483–488.
Morales, C.R., Oko, R., Clermont, Y., 1994. Molecular cloning and developmental expression of an mRNA encoding the 27 kDa outer dense fiber protein of rat spermatozoa. Mol. Reprod. Dev. 37, 229–240.
Nair, M., Teng, A., Bilanchone, V., Agrawal, A., Li, B., Dai, X., 2006. Ovol1 regulates the growth arrest of embryonic epidermal progenitor cells and represses c-myc transcription. J. Cell Biol. 173, 253–264.

Nam, S.Y., Maeda, S., Ogawa, K., Kurohmaru, M., Hayashi, Y., 1997. Expression pattern of the mitochondrial capsule selenoprotein mRNA in the mouse testis after puberty; in situ hybridization study. J. Vet. Med. Sci. 59, 983–988.

Nelson, J.E., Krawetz, S.A., 1993. Linkage of human spermatid-specific basic nuclear protein genes. Definition and evolution of the P1–>P2–>TP2 locus. J. Biol. Chem. 268, 2932–2936.

Parker, D.S., Jemison, J., Cadigan, K.M., 2002. Pygopus, a nuclear PHD-finger protein required for Wingless signaling in *Drosophila*. Development 129, 2565–2576.

Pena, P.V., Davrazou, F., Shi, X., Walter, K.L., Verkhusha, V.V., Gozani, O., Zhao, R., Kutateladze, T.G., 2006. Molecular mechanism of histone H3K4me3 recognition by plant homeodomain of ING2. Nature 442, 100–103.

Saunders, P.T., Millar, M.R., Maguire, S.M., Sharpe, R.M., 1992. Stage-specific expression of rat transition protein 2 mRNA and possible localization to the chromatoid body of step 7 spermatids by in situ hybridization using a nonradioactive riboprobe. Mol. Reprod. Dev. 33, 385–391.

Schwab, K.R., Patterson, L.T., Hartman, H.A., Song, N., Lang, R.A., Lin, X., Potter, S.S., 2007. Pygo1 and Pygo2 roles in Wnt signaling in mammalian kidney development. BMC Biol. 5, 15.

Shi, X., Hong, T., Walter, K.L., Ewalt, M., Michishita, E., Hung, T., Carney, D., Pena, P., Lan, F., Kaadige, M.R., Lacoste, N., Cayrou, C., Davrazou, F., Saha, A., Cairns, B.R., Ayer, D.E., Kutateladze, T.G., Shi, Y., Cote, J., Chua, K.F., Gozani, O., 2006. ING2 PHD domain links histone H3 lysine 4 methylation to active gene repression. Nature 442, 96–99.

Shirley, C.R., Hayashi, S., Mounsey, S., Yanagimachi, R., Meistrich, M.L., 2004. Abnormalities and reduced reproductive potential of sperm from Tnp1- and Tnp2-null double mutant mice. Biol. Reprod. 71, 1220–1229.

Song, N., Schwab, K.R., Patterson, L.T., Yamaguchi, T., Lin, X., Potter, S.S., Lang, R.A., 2007. pygopus 2 has a crucial, Wnt pathway-independent function in lens induction. Development 134, 1873–1885.

Stadeli, R., Basler, K., 2005. Dissecting nuclear Wingless signalling: recruitment of the transcriptional co-activator Pygopus by a chain of adaptor proteins. Mech. Dev. 122, 1171–1182.

Tanaka, H., Iguchi, N., Isotani, A., Kitamura, K., Toyama, Y., Matsuoka, Y., Onishi, M., Masai, K., Maekawa, M., Toshimori, K., Okabe, M., Nishimune, Y., 2005. HANP1/H1T2, a novel histone H1-like protein involved in nuclear formation and sperm fertility. Mol. Cell Biol. 25, 7107–7119.

Taverna, S.D., Ilin, S., Rogers, R.S., Tanny, J.C., Lavender, H., Li, H., Baker, L., Boyle, J., Blair, L.P., Chait, B.T., Patel, D.J., Aitchison, J.D., Tackett, A.J., Allis, C.D., 2006. Yng1 PHD finger binding to H3 trimethylated at K4 promotes NuA3 HAT activity at K14 of H3 and transcription at a subset of targeted ORFs. Mol. Cell 24, 785–796.

Thompson, B.J., 2004. A complex of Armadillo, Legless, Pygopus coactivates dTCF to activate wingless target genes. Curr. Biol. 14, 458–466.

Thompson, B., Townsley, F., Rosin-Arbesfeld, R., Musisi, H., Bienz, M., 2002. A new nuclear component of the Wnt signalling pathway. Nat. Cell Biol. 4, 367–373.

Townsley, F.M., Cliffe, A., Bienz, M., 2004. Pygopus and Legless target Armadillo/beta-catenin to the nucleus to enable its transcriptional co-activator function. Nat. Cell Biol. 6, 626–633.

Tsunekawa, N., Matsumoto, M., Tone, S., Nishida, T., Fujimoto, H., 1999. The Hsp70 homolog gene, Hsc70t, is expressed under translational control during mouse spermiogenesis. Mol. Reprod. Dev. 52, 383–391.

van der Hoorn, F.A., Tarnasky, H.A., Nordeen, S.K., 1990. A new rat gene RT7 is specifically expressed during spermatogenesis. Dev. Biol. 142, 147–154.

Veeman, M.T., Axelrod, J.D., Moon, R.T., 2003. A second canon. Functions and mechanisms of beta-catenin-independent Wnt signaling. Dev. Cell 5, 367–377.

Vernet, N., Dennefeld, C., Rochette-Egly, C., Oulad-Abdelghani, M., Chambon, P., Ghyselinck, N.B., Mark, M., 2006. Retinoic acid metabolism and signaling pathways in the adult and developing mouse testis. Endocrinology 147, 96–110.

Vornberger, W., Prins, G., Musto, N.A., Suarez-Quian, C.A., 1994. Androgen receptor distribution in rat testis: new implications for androgen regulation of spermatogenesis. Endocrinology 134, 2307–2316.

Wu, J.Y., Means, A.R., 2000. Ca(2+)/calmodulin-dependent protein kinase IV is expressed in spermatids and targeted to chromatin and the nuclear matrix. J. Biol. Chem. 275, 7994–7999.

Wysocka, J., Swigut, T., Xiao, H., Milne, T.A., Kwon, S.Y., Landry, J., Kauer, M., Tackett, A.J., Chait, B.T., Badenhorst, P., Wu, C., Allis, C.D., 2006. A PHD finger of NURF couples histone H3 lysine 4 trimethylation with chromatin remodelling. Nature 442, 86–90.

Yomogida, K., Ohtani, H., Harigae, H., Ito, E., Nishimune, Y., Engel, J.D., Yamamoto, M., 1994. Developmental stage- and spermatogenic cycle-specific expression of transcription factor GATA-1 in mouse Sertoli cells. Development 120, 1759–1766.

Zhang, F.P., Hamalainen, T., Kaipia, A., Pakarinen, P., Huhtaniemi, I., 1994. Ontogeny of luteinizing hormone receptor gene expression in the rat testis. Endocrinology 134, 2206–2213.

Zhao, M., Shirley, C.R., Hayashi, S., Marcon, L., Mohapatra, B., Suganuma, R., Behringer, R.R., Boissonneault, G., Yanagimachi, R., Meistrich, M.L., 2004. Transition nuclear proteins are required for normal chromatin condensation and functional sperm development. Genesis 38, 200–213.